

Surface nematic bistability at nanoimprinted topography

Jin Seog Gwag,^{1,a)} Jae-Hoon Kim,² Makoto Yoneya,³ and Hiroshi Yokoyama³

¹Liquid Crystal Nano-System Project, ERATO-SORST, Japan Science and Technology Agency, Tokodai, Tsukuba, Ibaraki 300-2635, Japan; Research Institute of Information Display, Hanyang University, Seoul 133-791, Republic of Korea

²Research Institute of Information Display, Hanyang University, Seoul 133-791, Republic of Korea

³Nanotechnology Research Institute, National Institute of Advanced Industrial Science and Technology 1-1-1 Umezono, Tsukuba, Ibaraki 305-8568, Japan

(Received 1 February 2008; accepted 31 March 2008; published online 15 April 2008)

The azimuthal nematic bistability was realized by frustration between two azimuthally orthogonal anchoring axes induced by a nanoimprinted groove pattern and mechanical rubbing. The nematic bistability can be explained by the revised Berreman model of groove-induced surface anchoring, recently introduced by Fukuda *et al.* [Phys. Rev. Lett. **98**, 187803 (2007)]. The azimuthal bistability can be tuned in arbitrary direction by changing the groove pitch and rubbing conditions. This simple combinatorial scheme may be considered as a practical candidate for bistable displays with tailored bistable directions required in various liquid crystal device modes. © 2008 American Institute of Physics. [DOI: 10.1063/1.2912038]

The alignment of liquid crystals (LCs) on solid substrates is important for practical applications such as display technologies as well as scientific understanding of surface ordering, surface transitions, or surface wetting. Surface treatments, such as obliquely evaporated SiO_x layers, Langmuir–Blodgett films, rubbed polymer films, and ultraviolet (UV) light or ion-beam exposed polymer films, have been used to obtain homogeneous alignment of LCs.^{1–10} As an alternative for such a LC alignment, anisotropic surface topography can lead to preferential orientation of LCs via the minimization of the Frank elastic energy.^{11–13} In contrast to those methods that only give monostable LC alignment on the treated substrates, bistable LC alignment has been studied for merits in display such as reduction of power consumption and increase of viewing angle.^{14–22} Beberi *et al.* have demonstrated the method to obtain in-plane bistable nematic anchoring conditions based on the principle of anchoring competition.²³ Yi *et al.* studied the nematic bistability at two-dimensional surface topography.¹⁴ We have also verified experimentally azimuthal nematic bistability at two-dimensional surface relief fabricated by nanoimprint lithography (NIL).²⁴ The most general model about the surface anchoring energy on microtopographical features was proposed by Berreman¹¹ and has been employed in many literatures. However, the Berreman's theory predicts the elastic anchoring energy proportional to $\sin^2 \phi$, with ϕ being the angle between the director and the direction of the surface grooves, which cannot explain the LC bistability observed

for such two-dimensional groove systems. Recently, Fukuda *et al.* reexamined the Berreman's theory and showed that the Berreman's result is not generally valid, reformulating a correct surface anchoring energy.²⁵ This model successfully explains the LC bistability in the two-dimensional groove system.

In this letter, we experimentally examine the validity of the model of Fukuda *et al.* In order to induce LC bistability, we used a combination of a groove pattern and mechanical rubbing having mutually orthogonal anchoring directions. This may be one of the simplest methods to get LC bistability by way of the control of surface LC director by modulation of the rubbing strength and/or the groove size. This combined surface alignment was made possible in our study by applying a new functionally gradient alignment layer material, the details of which have been described in a previous paper.²⁶

In our experiment, groove pattern was created by NIL. NIL has a capability to create microtopographical patterns with high throughput and high precision through a step and stamp process. It enables us to quantitatively control the surface anchoring by the decalcomania of a mold pattern with a definite pitch and depth to an LC alignment layer.^{27–29} In typical experiments, the solution of the hybrid-type polyimide (HPI), the functionally gradient material specifically designed for NIL and LC alignment. This material is featured by hybridization of two distinct moieties with largely different thermomechanical properties and surface activity. The

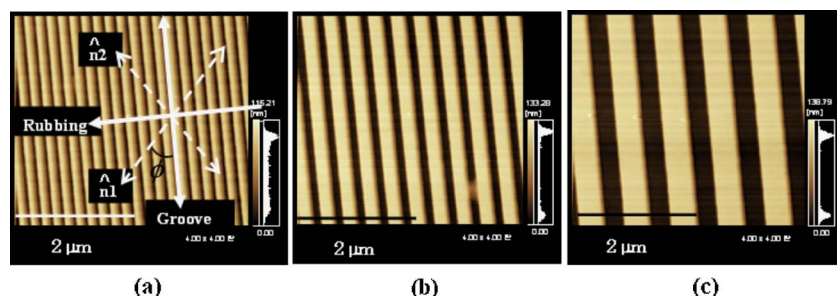


FIG. 1. (Color online) AFM image of the nano sized features which were transferred from a mold pattern into the hybrid type polyimide. The rubbing direction performed on the nano-pattern was indicated.

^{a)}Electronic mail: small3000@hotmail.com.

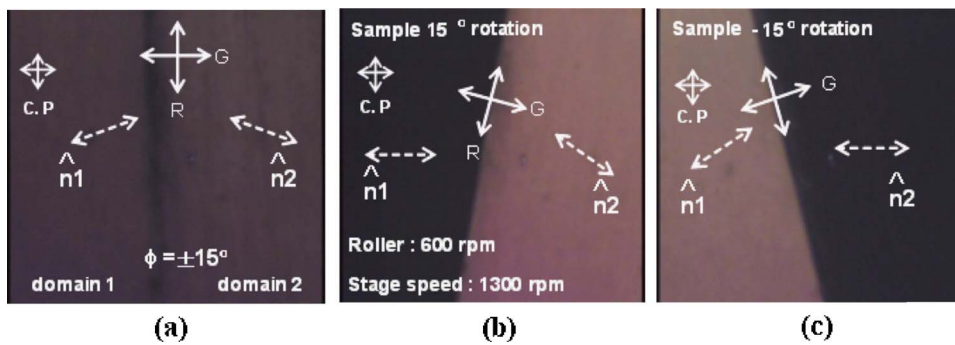


FIG. 2. (Color online) Polarizing microscopic images of nematic LCs dropt on the surface rubbed with the roller rotation of 600 rpm on a surface grooved by NIL: (a) when the groove direction denoted by G was placed on optically transmissive axis of a polarizer in the crossed polarizers, (b) when the groove direction is put on 15° , and (c) when the groove direction is put on -15° .

bulk layer of this HPI film mostly has the characteristics of epoxy resin; however, the surface layer is dominantly covered by the polyimide. While the polyimide layer functions as an excellent LC alignment layer with rubbing, the layer made from the epoxy resin and polyesteramic acid is suitable for NIL. Fabricating and imprinting conditions of HPI film have been introduced in previous papers.^{24,26}

Figure 1 shows atomic force microscopy (AFM) (SPM-9500J3, Shimadzu Corp.) images of nanosized features having different pitches that were transferred from the mold patterns. The pitches of the patterns of Figs. 1(a)–1(c) were 200, 400, and 800 nm, respectively, with their depths being constant at 120 nm. The rubbing performed in our experiment leads to azimuthally orthogonal anchoring direction with respect to the anisotropic anchoring direction generated by the groove.

To control the anchoring strength by rubbing, we changed the number of rotation of the rubbing roller, which is easier to change than the other rubbing parameters.³⁰ Figure 2 shows the polarizing microscopic images of the LC cell filled with 4-n-pentyl-4'-cyanobiphenyl LC on the rubbed surface with 400 nm pitch groove. Here, the rubbing conditions were as follows. The roller rotation was 600 rpm, the rubbing depth was 3 mm, and the stage speed 30 mm/s. The counter substrate was coated with a homeotropic LC alignment layer, polyimide SE-1211 from Nissan Chemical Corp., to observe more clearly LC bistability in the cell. Figure 2(a) is a polarizing optical microscopic image, when either the rubbing or groove direction was fixed along the optical axis of a polarizer in the crossed polarizers-configuration. Under this optical condition, we cannot distinguish the two stable domains except for linear discrimination line at the central part

of this figure. If we rotate, however, the LC cell by 15° from Fig. 2(a), as shown in Fig. 2(b), then we can clearly demarcate the two domains and know the LC direction of the left domain through the extinction direction of the left domain. In the same way, when the rubbing axis is set at -15° with respect to optically transmissive axis of a polarizer as shown in Fig. 2(c), we are able to tell the LC direction of the right domain. Two distinct and equivalent stable directions have symmetry with respect to the groove direction.

Figure 3 shows the variations of the bistable LC direction as a function of the rubbing-induced anchoring strength measured in terms of the rotation speed of rubbing roller for various groove pitch, $\lambda=200, 400,$ and 800 nm. On the groove with $\lambda=200$ nm, the orientation remains along the groove up to the highest rubbing speed, indicating the dominance of the groove contribution over the rubbing-induced anchoring. In this case, the angular deviation from the groove remained less than that existed within 5° because the anchoring strength by groove is much larger than that by rubbing (the relative anchoring $g \sim 1/64$). By increasing the pitch to reduce the groove anchoring, however, there occurs a conspicuous variation of the easy axis as a function of rubbing condition. At the pitch of 800 nm, we find from Figs. 2 and 4 that $\phi \sim 50^\circ$, which corresponds to nearly equal anchoring strengths, i.e., $g=1$. Therefore, we can also know that the azimuthal anchoring energy for rubbing in this system corresponds to it by groove's pitch of 800 nm. In case of pitch of 400 nm, ϕ distributes between 10° and 22° depending on rubbing strength.

According to the Fukuda model,²⁵ the total free energy density at this surface, including the rubbing contribution, is given by

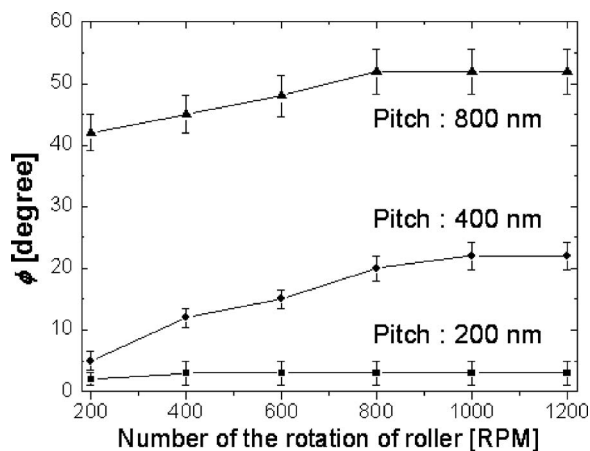


FIG. 3. Bistable nematic LC direction observed on several rotations of rubbing roller with respect to groove's pitch 200, 400, and 800 nm.

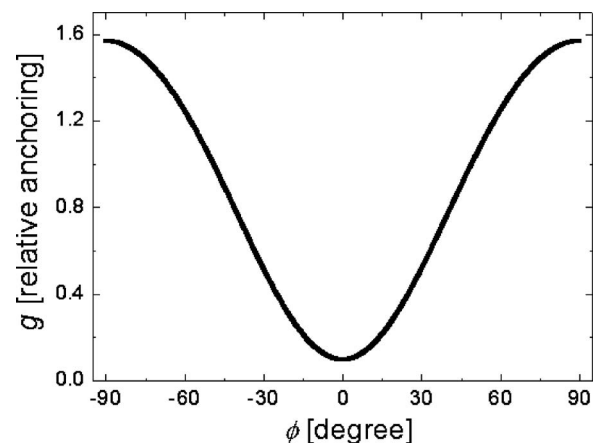


FIG. 4. Nematic LC bistability depending on the relative anchoring strength.

$$F_d = \frac{1}{2} W_G \frac{\sin^2 \phi}{\sqrt{\cos^2 \phi + \beta_1 \sin^2 \phi}} \left[\sin^2 \phi + \beta_3 \cos^2 \phi \left(2 - \beta_3 \frac{\sqrt{\cos^2 \phi + \beta_1 \sin^2 \phi} \sqrt{\cos^2 \phi + \beta_2 \sin^2 \phi} - \cos^2 \phi}{\sin^2 \phi} \right) \right] - \frac{1}{2} W_R \sin^2 \phi. \quad (1)$$

Here, ϕ is the angle between the director and the direction of the surface grooves and $\beta_1 = K_{33}/K_{11}$, $\beta_2 = K_{33}/K_{22}$, $\beta_3 = (K_{22} + K_{24})/K_{33}$, and $W_G = 1/2 K_3 A^2 (2\pi/\lambda)^3$, where K_{11} , K_{22} , K_{33} , and K_{24} are the splay, twist, bend, and splay-bend surface elastic constants, respectively, and A and λ are the amplitude and pitch of the groove. W_R represents the anchoring strength by the rubbing, for which we assume the Rapini-Papoular form. One should note, here, that in the absence of surface elastic contribution ($\beta_3 = 0$), the anchoring energy by surface groove is proportional to $\sin^4 \phi$ rather than to $\sin^2 \phi$ as in the original Berreman's model.

The stable orientations on this frustrated surface should satisfy

$$\frac{dF_d(\phi)}{d\phi} = 0. \quad (2)$$

$g = W_R/W_G$, relative anchoring strength between the two orthogonal alignment as the function of ϕ can be led from Eq. (2). From the experimental results of Fig. 3, we can determine $\beta_3 \approx 0.05$, which means $k_{24} \approx -0.9k_{22}$ for $\beta_1 = 1.3$ and $\beta_2 = 2.2$.³¹ In general, the range of k_{24} is known as $-k_{22} \leq k_{24} \leq k_{22}$. Then, we plot g as the function of ϕ to check the bistability dependence on the relative anchoring strength, as shown in Fig. 4. For $W_G \geq W_R$, bistability exists always except $g = 0$. However, for $W_G \leq W_R$, bistability is limited in the condition of $g < 1.57$. It implies that $\sin^2 \phi$ contribution dominantly affects in this system, comparing with that of $\sin^4 \phi$. As in Fig. 3, we found the bistability in all cases we have tried. These experimental results show validity of the Fukuda model at LC system with such a surface grating.

The relative anchoring strength can be precisely controlled through tuning the groove pitch by one-step NIL and rubbing conditions to get the bistable direction required in various liquid crystals display (LCD) application areas. For example, the bistable direction of 45° and -45° can be applied to transmissive type LCD mode with in-plane switching, having very excellent optical characteristics like in-plane switching mode or fringe field switching mode. On the other hand, 22.5° and -22.5° bistability may be appropriate for reflective type or transfective type LCD modes with in-plane switching or vertical switching.

In summary, an azimuthal nematic bistability can be produced by the combination of a nanoimprinted groove pattern and a mechanical rubbing. Applying the new functionally gradient alignment layer material enabled this combination. The experimental results are well explained by the Fukuda's model. In principle, azimuthal bistability of any directions can be obtained by the modulation of groove pitch and rubbing conditions. Therefore, this simple combination may be

considered as a candidate for bistable display with tailored bistable directions required in various LC modes.

The authors thank Mr. H. Sato of Chisso Petrochemical Co. for providing the polyimide sample and Mr. K. Shimmo of Nippon Sheet Glass Co., Ltd. for providing nanoimprinted mold.

¹J. L. Janning, *Appl. Phys. Lett.* **21**, 173 (1972).

²M. Nakamura and M. Ura, *J. Appl. Phys.* **52**, 210 (1972).

³W. M. Gibbons, P. J. Shannon, S. T. Sun, and B. J. Swetlin, *Nature (London)* **351**, 49 (1991).

⁴N. Kawatsuki, T. Yamamoto, and H. Ono, *Appl. Phys. Lett.* **74**, 935 (1999).

⁵M. Schadt, H. Seiberle, and A. Schuster, *Nature (London)* **381**, 212 (1996).

⁶J.-H. Kim, S. Kumar, and S.-D. Lee, *Phys. Rev. E* **57**, 5644 (1998).

⁷J. Congard, *Mol. Cryst. Liq. Cryst. Suppl. Ser.* **A5**, 1 (1982).

⁸P. Chaudhari, *Nature (London)* **411**, 56 (2001).

⁹J. S. Gwag, C. G. Jhun, J. C. Kim, T.-H. Yoon, G.-D. Lee, and S. J. Cho, *J. Appl. Phys.* **96**, 257 (2004).

¹⁰J. S. Gwag, K.-H. Park, D. J. Kang, T.-H. Yoon, and J. C. Kim, *Jpn. J. Appl. Phys., Part 2* **42**, L468 (2003).

¹¹D. W. Berreman, *Phys. Rev. Lett.* **28**, 1683 (1972).

¹²H. Yokoyama, in *Handbook of Liquid Crystal Research*, edited by P. J. Collings and J. S. Patel (Oxford University Press, New York, 1997), Chap. 6.

¹³P. G. de Gennes and J. Prost, *The Physics of Liquid Crystals*, 2nd ed. (Oxford University Press, Oxford, 1993).

¹⁴Y. Yi, M. Nakata, A. R. Martin, and N. A. Clark, *Appl. Phys. Lett.* **90**, 163510 (2007).

¹⁵J. H. Kim, M. Yoneya, and H. Yokoyama, *Nature (London)* **420**, 159 (2002).

¹⁶J. H. Kim, M. Yoneya, J. Yamamoto, and H. Yokoyama, *Appl. Phys. Lett.* **78**, 3055 (2001).

¹⁷R. Barberi and G. Durand, in *Handbook of Liquid Crystal Research*, edited by P. J. Collings and J. S. Patel (Oxford University Press, New York, 1997), Chap. 15.

¹⁸R. Barberi and G. Durand, *Appl. Phys. Lett.* **58**, 2907 (1991).

¹⁹I. Dozov, M. Nobili, and G. Durand, *Appl. Phys. Lett.* **70**, 1179 (1997).

²⁰D.-K. Yang, J. L. West, L. C. Chien, and J. W. Doane, *J. Appl. Phys.* **76**, 1331 (1994).

²¹N. A. Clark and S. T. Lagerwall, *Appl. Phys. Lett.* **36**, 899 (1980).

²²D. W. Berreman and W. R. Heffner, *Appl. Phys. Lett.* **37**, 109 (1980).

²³R. Barberi, J. J. Bonvent, M. Giocondo, M. Iovane, and A. L. Alexe-Ionescu, *J. Appl. Phys.* **84**, 1321 (1998).

²⁴J. S. Gwag, J. Fukuda, M. Yoneya, and H. Yokoyama, *Appl. Phys. Lett.* **91**, 073504 (2007).

²⁵J. Fukuda, M. Yoneya, and H. Yokoyama, *Phys. Rev. Lett.* **98**, 187803 (2007); **99**, 039902 (2007).

²⁶J. S. Gwag, M. Oh-e, M. Yoneya, H. Yokoyama, H. Satou, and S. Itami, *J. Appl. Phys.* **102**, 063501 (2007).

²⁷M. Berggren, A. Dodabalapur, R. E. Slusher, A. Timko, and O. Nalamasu, *Appl. Phys. Lett.* **72**, 410 (1998).

²⁸S. Y. Chou, P. R. Krauss, and P. J. Renstrom, *Science* **272**, 85 (1996).

²⁹O. Hayden and F. L. Dickert, *Adv. Mater. (Weinheim, Ger.)* **13**, 1480 (2001).

³⁰D.-S. Seo and S. Kobayashi, *Appl. Phys. Lett.* **66**, 1202 (1995).

³¹M. Cui and J. R. Kelly, *Mol. Cryst. Liq. Cryst. Sci. Technol., Sect. A* **331**, 49 (1999).